Structure and composition of layers of Ni-Co-Mn-In Heusler alloys obtained by pulsed laser deposition

Grzegorz Wisz[1,*], *Piotr* Sagan[2], *Ireneusz* Stefaniuk[3], *Bogumil* Cieniek[1], *Wojciech* Maziarz[4], and *Marian* Kuzma[2]

[1]Faculty of Mathematics and Natural Sciences, Department of Experimental Physics, University of Rzeszow, Pigonia 1, 35-959 Rzeszow, Poland
[2]Faculty of Mathematics and Natural Sciences, Department of Biophysics, University of Rzeszow, Pigonia 1, 35-959 Rzeszow, Poland
[3]Faculty of Mathematics and Natural Sciences, Center for Microelectronics and Nanotechnology, University of Rzeszow, Pigonia 1, 35-959 Rzeszow, Poland
[4]Institute of Metallurgy and Materials Science of the Polish Academy of Science, 25 Reymonta Str., 30-059 Krakow, Poland

Abstract. In present work we were analysing thin layers of Ni-Co-Mn-In alloys, grown by pulsed laser deposition method (PLD) on Si, NaCl and glass substrates. For target ablation the second harmonics of YAG:Nd^{3+} laser was used. The target had the composition $Ni_{45}Co_5Mn_{34.5}In_{14.5}$. The morphology of the layers and composition were studied by electron microscopy TESCAN Vega3 equipped with microanalyzer EDS – Easy EdX system working with Esprit Bruker software. The X-ray diffraction measurements (XRD), performed on spectrometer Bruker XRD D8 Advance system, reveals Ni_2-Mn-In cubic phase having lattice constant a = 6.02Å.

1 Introduction

A phenomenon of a giant magnetoresistance (GMR) and a phenomenon of a tunnel magnetoresistance (TMR) in structures of a magnetic layer/layer of metal (or a dielectric) /magnetic layer are used for spintronics purposes. Heusler alloys which base on Mn-Ge [1, 2], Mn-Si [3] or CoMnSi [4] are very promising. Nevertheless, other multifunctional Heusler alloys having nonordinary properties like high perpendicular magnetic anisotropy, low damping constant or half-metallicy could be useful in spintronic as well [5]. The growth and investigation of thin layers of such materials are highly desired step for future applications in field of spintronics. NiMnIn belongs to the separate group of Heusler alloys called metamagnetic alloys (NiMnGa, NiMnSn, NiMnIn) [6]. The strong magnetic and structural nonhomogeneity in this compound may be the source of GMR[7].

In this paper we grown thin layers from bulk $Ni_{50-y}Co_yMn_{50-x}In_x$ (y=5,

* Corresponding author: gwisz@ur.edu.pl

x=14.5). Addition of Co into NiMnIn moves the Curie temperature to the region of room temperature or higher [8]. We have applied pulsed laser deposition method (PLD) [9] for layers fabrication, which is a low temperature method what ensures the abrupt interfaces [10]. Moreover, PLD is non equilibrium method what can maintain the composition of the target in the layer [11].

2 Experimental

The NiCoMnIn films on silicon, glass and NaCl substrates were deposited by PLD using the YAG: Nd^{3+} laser with the 532 nm (II harmonics) wavelength, 6 ns pulse time, 10Hz repetition rate and fluence F in the range 16 J/cm^2. The bulk $Ni_{50-x}Co_xMn_{35.5}In_{14.5}$ was used as a target [12]. The laser beam was focused on the target using a quartz lens with focal distance of 600 mm. The growth temperature T_s was kept at 20^{O}C – 200^{O}C and the deposition of the layers was carried out at 10^{-7} mbar vacuum. The samples list and technological parameters contains Table 1.

Table 1. List of PLD samples and technological parameters.

No.	Substrate	Substrate temperature [K]	Process time [min]	Vacuum [mbar]	Analysis
P1	Si, Glass, Al_2O_3	293	15	$1.9*10^{-7}$	
P2	Si, NaCl, Glass	305	20	$2.4*10^{-7}$	EDS, SEM
P3	Si, NaCl, Glass	473	20	$1.6*10^{-7}$	
P4	Si, NaCl, Glass	302	10	$1.48*10^{-7}$	
P5	Si, NaCl, Glass	303.6	30	$1.48*10^{-7}$	
P6	Si, NaCl, Glass	301.2	30	$1.01*10^{-7}$	EDS, SEM, XRD
P7	Si, NaCl, Glass	301.1	10	$7.07*10^{-8}$	EPR
P8	Si, NaCl, Glass, N2"Wh	373	30	$1.16*10^{-7}$	XRD

Composition and morphology of the films were investigated by scanning electron microscope Tescan Vega3, which was equipped in energy dispersive X-ray spectroscopy (EDS) analyser. The X-ray diffraction study was performed on spectrometer Brucker XRD D8 Advance System.

3 Results and discussion

3.1 Morphology and composition

The obtained layers are very smooth by visual inspection. SEM microscopy observations (Fig. 1b) confirm this statement. The thickness of the sample was determined on about 75 nm based on the edge of the breaking sample shown in Fig. 1a. Many regular drops were observed on the surface. The size of drops is 0.5 - 2 μm. Such existence of drops is typical for layers obtained by PLD. In Fig. 1c a very regular shape (as ball) of one exceptional great drop is presented.

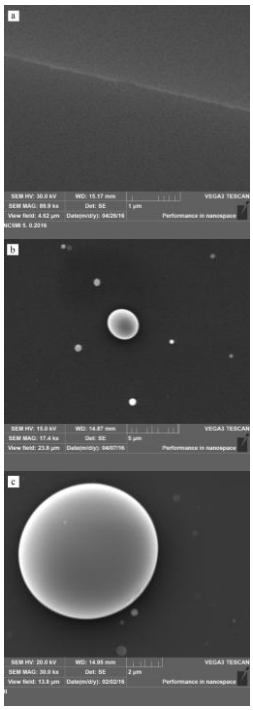

Fig. 1. SEM images of the layer P6 at small (a) and great magnification (b). Shape of the great drop (c).

Composition of layers was measured by EDS at low accelerating voltage due to small thickness of the films. In Fig. 3. results obtained at 5 kV and 10kV were compared. One can notice fair convergence of both results. In Table 2 the results of particular measurements were collected. From these data the average value was calculated. The thickness of layer is much smaller than the excitation area therefore the amount of Si is greater and accuracy of measure is lower. The composition of drop (shown in Fig. 1c) is determined with better accuracy while the diameter is greater than the size of excitation area (small amount of Si substrate in account).

Table 2. Composition at at. % of the layer P6 and the drop in it.

	5kV		10kV		Average composition of the layer
	Layer P6		Layer P6	Drop	
	without Si	with Si	with Si	with Si	
Si	-	37.26	84.93	1.52	61.10
Ni	69.57	67.41	65.83	54.73	67.60
Co	1.71	1.80	2.85	1.70	2,12
Mn	22.62	23.37	24.95	34.33	23.65
In	6.09	7.43	6.44	9.23	6.65

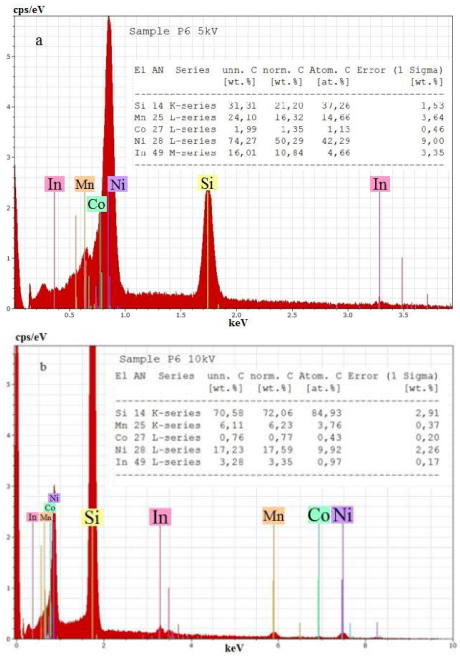

Fig. 2. Composition measured at 5 kV (a) and at 10 kV (b).

3.2 XRD analysis

In Fig. 3. X-ray diffraction patterns for samples P6 and P8 deposited on (001)Si at substrate temperature 301,2K and 373K respectively were shown. The diffraction lines are very weak due to thinness of layers. Only the reflex from Si substrate (at $2\theta = 69.325^{o}$) is very strong therefore, the intensity axis is given with logarithmic scale. Both spectra are characteristic for polycrystalline samples and do not differ considerably, so we analyse one of them: for sample P6 which was grown at room temperature. The 2θ values of diffraction lines for this sample (P6) are presented in Fig. 4. and in Table 3.

In Table 3 the parameters (2θ, intensity and hkl) of diffraction lines are collected for experimental spectrum from Fig. 4. and for more possible phases of metallic Ni (cubic), Mn (cubic) and In (cubic). Moreover there are diffraction lines of stoichiometric Ni_2MnIn and nonstoichiometric $Ni_2Mn_{1-x}In_x$ x=0.05. The best relation of some experimental diffraction lines to the database lines is for stoichiometric Ni_2MnIn. A small amount of one component cubic Ni and Mn should be considered as well.

The system of the diffractometer identify the spectrum as Ni_2MnIn using ICDD PDF-2 2012 database (see lower part in Fig. 4. and Fig. 5.c). This compound relates to the phase $Ni_{50}Mn_{50-x}In_x$, x=25 analysed by T. Krenke et all. [13] (Fig. 5b). Lattice constant for our phase is a = b = c = 6.02Å whereas, Krenke determined the lattice constant for $Ni_{50}Mn_{50-x}In_x$, x=25 a = b = c = 6.071Å. This discrepancy can be explained by nonstoichiometry. By replacing In with Mn the lattice constant of the austenitic phase become smaller. Taking into account the dependence of lattice constant on composition (see Fig. 6.) the composition $Ni_2Mn_{1+y}In_{1-y}$ for lattice constant 6.02Å is $y = 0.22 \pm 0.02$ and depends on magnetic ordering [14] what is considered in accuracy Δy. This value relates to x = 19.5.

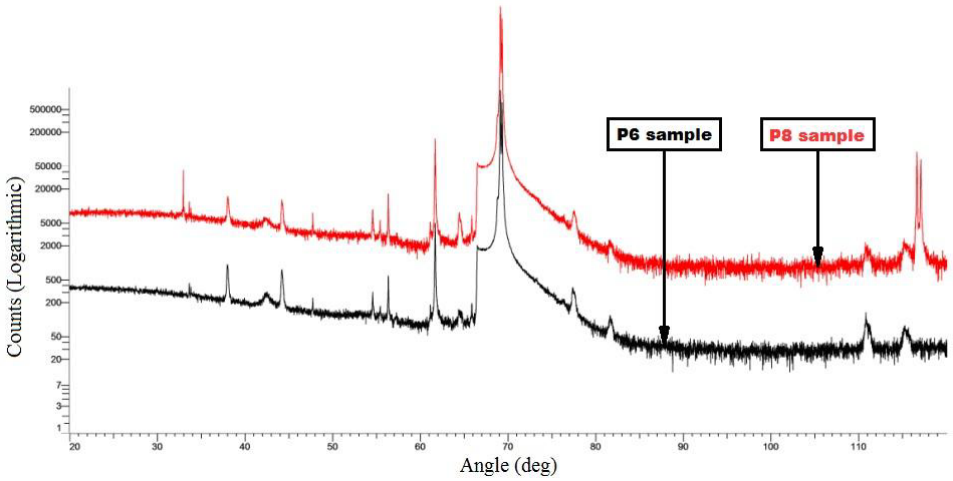

Fig. 3. X-ray diffraction patterns for samples P6 and P8.

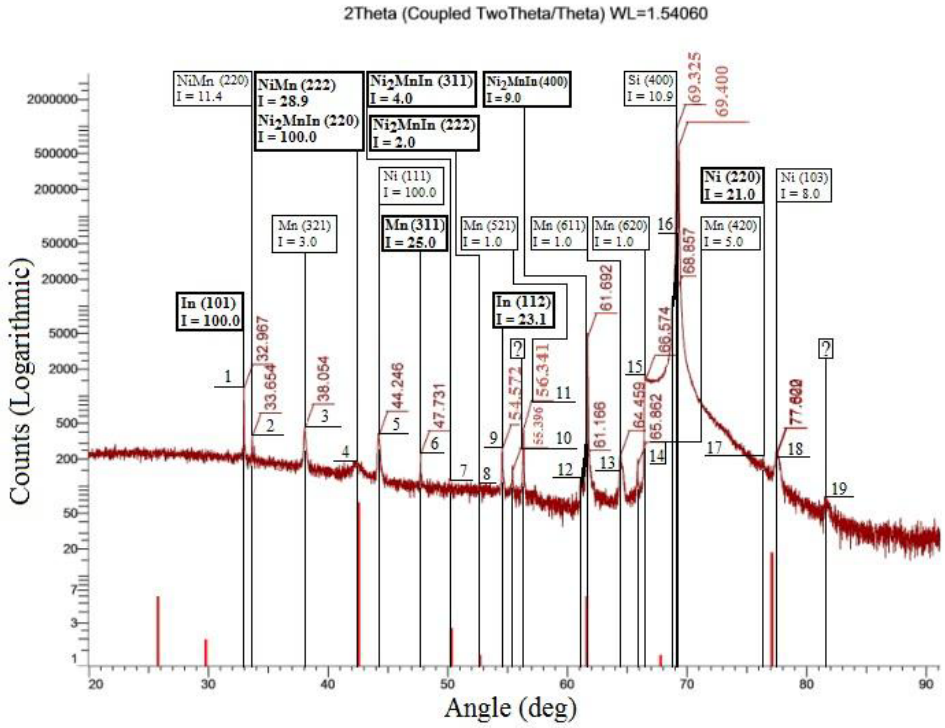

Fig. 4. X-ray diffraction pattern for sample P6 and the scheme of reference diffraction lines of phases Ni(cub), Mn(cub), In, NiMn, Ni_2MnIn (according to the Table 3).

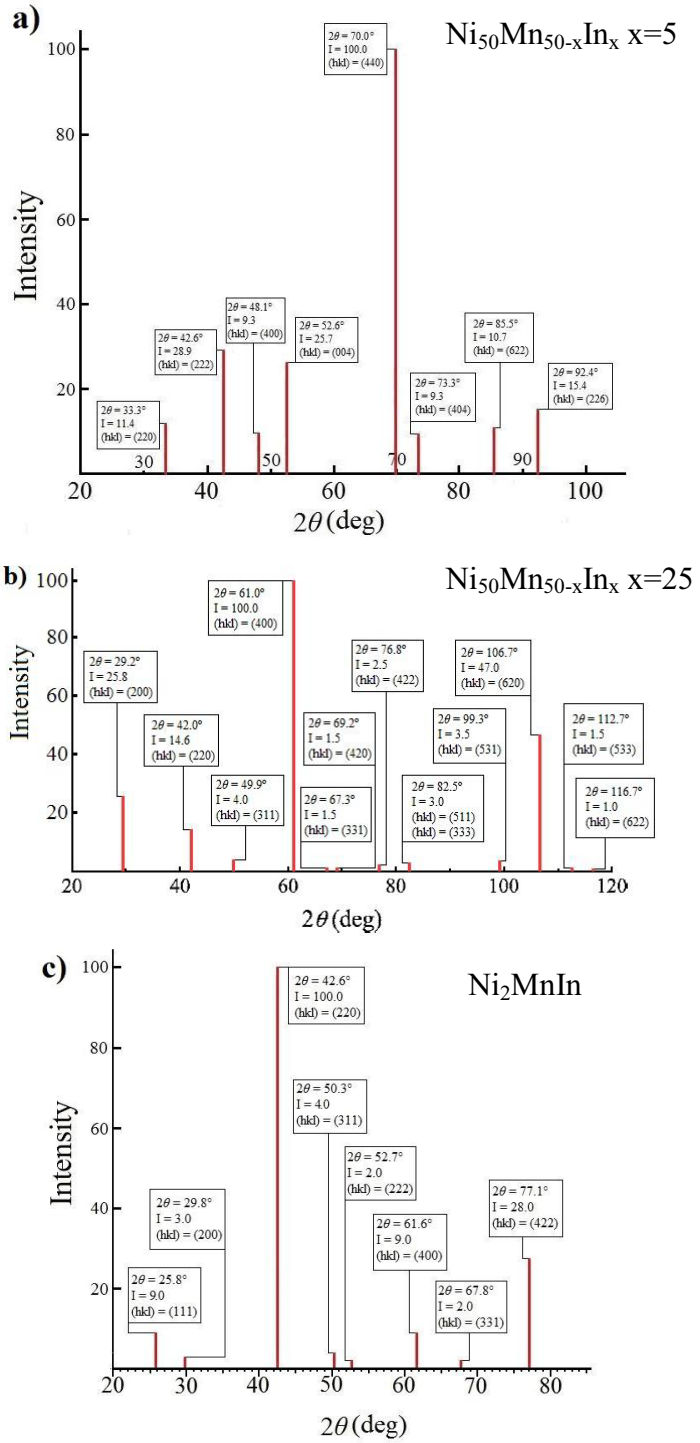

Fig. 5. X-ray diffraction lines of $L1_0$ phase of $Ni_{50}Mn_{50-x}In_x$, x=5 (according to Fig. 6. of [13]) (a), $L2_1$ phase of $Ni_{50}Mn_{50-x}In_x$, x=25 (according to Fig. 3. of [13]) (b), $L2_1$ phase of Ni_2MnIn, (according to ICDD PDF-2 database) (c).

Table 3. Relations of the position of the database XRD lines of metallic Ni,Mn,In and Ni_2MnIn, $Ni_2Mn_{1-x}In_x$ x=0.05 compounds with experimental diffraction pattern of the sample P6.

Experimental			ASTM						database.iem.ac.ru/mincryst/			ICDD PDF-2 database, pattern: PDF 00-040-1208			Krenke et all. [13]		
			CAS num: 7440-02-0			CAS num: 7439-96-5											
			Ni(c)			Mn(c)			In(c)			Ni2MnIn			$NiMnIn_x$ x=0.05		
line	2Θ	I	2Θ	I	hkl	2Θ	I	hkl	2Θ	I	hkl	2Θ	I	hkl	2Θ	I	hkl
1.	32.967	m							33.010	100	(101)						
2.	33.654	w	37.735	3.0	(321)										33.3	11.4	(220)
3.	38.054	w															
4.	42.500	vw										42.570	100	(220)	42.6	28.9	(222)
5.	44.246	w	44.505	100	(111)												
6.	47.731	w				47.728	25.0	(311)									
7.	50.300	vw										50.315	4.0	(311)			
8.	52.700	vw										52.716	2.0	(222)	52.6	25.7	(004)
9.	54.572	w							54.563	23.1	(112)						
10.	55.396	vw	Weak, unidentified line.														
11.	56.341	m				56.502	1.0	(521)									
12.	61.166 61.692	s										61.617	9.0	(400)			
13.	64.459	w				64.378	1.0	(611)									
14.	65.862	w				66.149	5.0	(420)									
15.	66.574	m				66.292	1.0	(620)									
16.	68.857 69.325 69.400	vs							69.250	11.0	(202)						
17.	76.400	vw	76.366	21.0	(220)												
18.	77.600	w	78.000	8.0	(103)												
19.	81.600	vw	Weak, unidentified line.														

vw - very week w - week m - medium s - strong vs - very strong

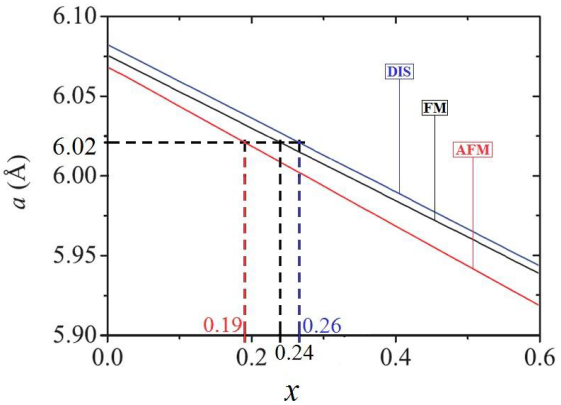

Fig. 6. Dependence of lattice constant of $L2_1$ $Ni_2Mn_{1+y}In_{1-y}$ on composition (according to Fig.2. of [14]) for different magnetic phases: ferromagnetic (FM), antiferromagnetic (AFM) and disordered (DIS).

4 Conclusions

1. Thin layers (~75 nm) on Si substrate have been grown by PLD method from target $Ni_{45}Co_5Mn_{35,5}In_{14,5.}$
2. EDS study revealed that the films have composition similar to the composition of target. However, the excess of Ni in respect to Mn were observed.
3. XRD measurments point on $Ni_2CoMnIn$ cubic phase with lattice constant a = 6.02 Å. This correspond to the composition x = 0.22 of the $L2_1$ $Ni_2Mn_{1+x}In_{1-x}$.

References

1. V.A. Oksenenko, L.N. Trofimova, Yu.N. Petrov, Y.V. Kudryavtsev, J. Dubowik, Y.P. Lee, Journal of Applied Physics **99**, 063902 (2009)
2. A. Sugihara, K. Suzuki, S. Mizukami, T. Miyazaki, J. Phys. D: Appl. Phys. **48**, 164009 (2015)
3. S. Zhou, K. Potzger, G. Zhang, A. Mücklich, F. Eichhorn, N. Schell, R. Grötzschel, B. Schmidt, W. Skorupa, M. Helm, J. Fassbender, Phys. Rev. B **75** 085203 (2007)
4. R. Fetzer et al, J. Phys. D: Appl. Phys. **48**, 164002 (2015)
5. S. Mizukami, A. Serga, J. Phys. D: Appl. Phys. **48**, 160301 (2015)
6. R. Kainuma, K. Oikawa, W. Ito, Y. Sutou, T. Kanomata, K. Ishida, J. Mater. Chem. **18**, 1873-1842 (2008)
7. I. Dubenko, A.K. Pathak, S. Stadler, N. Ali, Phys. Rev. B **80**, 092408 (2009)
8. H.C. Xuan, F.H. Chen, P.D. Han, D.H. Wang, Y.W. Du, Intermetallics **47**, 31-35 (2014)
9. D. B. Chrisey, G.K. Hubler, *Pulsed Laser Deposition of Thin Films,* Wiley & Sons, New York, 1994
10. S. Rai, M.K. Tiwari, G.S. Lodha, M.H. Hodi, M.K. Chattopadhyay, S. Majumdar, S. Gardelis, Z. Viskadourakis, J. Giapintzakis, R.V. Nandedkar, S.B. Roy, P. Chaddah, Phys. Review B **73**, 0354017 (2006)
11. J. T. Cheung and H. Sankur, CRC Crit. Rev. Solid State Matter. Sci. **15**, 63 (1988)
12. W. Maziarz, Solid State Phenomena **186**, 251-254 (2012)
13. T. Krenke, M. Acet, E.F. Wassermann, Phys. Rev. B **73**, 174413 (2006)
14. Ch.M. Li, H.B. Luo, Q.M. Hu, R. Yang, B. Johansson, L. Vitos, Phys. Rev. B **86**, 214205 (2012)